JMEPEG (2006) 15:445-452
DOI: 10.1361/105994906X117288

1059-9495/$19.00

Selection and Surface Treatment of Alloys in Solid Oxide Fuel Cell Systems

S. Elangovan, S. Balagopal, J. Hartvigsen, I. Bay, D. Larsen, M. Timper, and J. Pendleton

(Submitted January 16, 2006; in revised form May 22, 2006)

Cost and performance considerations determine the selection of various component materials in a solid oxide fuel cell power system. While the use of commercial alloys provides an opportunity for cost reduction, the requirements of different components vary widely. The interconnect materials must provide low electrical resistance while isolating the oxidizing and reducing gases. The air preheat and heat-exchanger components face high-temperature oxidizing conditions, while the fuel feed and reformer sections encounter highly reducing atmospheres that may contain varying levels of sulfur and CO, and thus are prone to sulfidation and metal dusting. Thus, each of the components requires both a judicious selection of the alloy composition and appropriate surface treatments. Coating processes were developed for two classes of alloy materials for potential use as interconnects and fuel feed hardware or process piping.

Keywords: conductive oxide scale, fuel cell interconnects, solid oxide fuel cell interconnect characterization, stainless steel separator, surface treatment

1. Introduction

To achieve commercial cost targets, solid oxide fuel cell (SOFC) development must take an integrated, multifaceted approach that includes system simplicity, performance improvement, and the use of low-cost materials and fabrication processes. The operating temperature range of SOFCs allows for both thermal and physical integration of high-temperature processes. By integrating the SOFC stack, hydrocarbon fuel reformer, and the air heat exchanger, overall system simplicity is attained resulting in a compact, low-cost system. Performance improvement is achieved by the use of cell designs such as anode-supported thin electrolyte cells or through the use of high-conductivity electrolyte materials. Although economy of scale is often considered critical to achieving acceptable target costs, the time lag between technology readiness and market introduction and acceptance makes it essential that low-cost materials options be considered during the development stage. It is thus essential to use materials, wherever possible, that are presently available commercially. However, it is recognized that modifications to the materials may be necessary to suit the operating conditions of the SOFCs.

Alloy materials suitable for high-temperature components have been widely used in a variety of technologies and provide a basis for the selection of various SOFC components. In fact, a number of stack components, such as interconnects, in one variation of cell design the porous cell support, and the gas manifolds can be made of metallic materials. In addition, alloys are well-suited for most of the balance of plant components, such as the air preheat, heat exchanger, the reformer housing, gas feed tubes, and the fuel gas humidifier. Thus, in a "ceramic" fuel cell, >90% of the components, both by weight and volume, can be made of metal.

The performance requirements of each of the components vary significantly. The interconnect faces the most stringent requirements and thus has demanded much of the recent research focus (Ref 1). The basic development objectives include simultaneously balancing physical constraints (i.e., thermal expansion match to other components, creep resistance at temperature, and oxide scale adhesion with time and thermal cycles,), chemical constraints (i.e., limited oxide scale growth rate in air and fuel, no evaporation of species that would poison the electrodes, and avoiding reactivity with electrode or contact material that would form insulating phases), electrical constraints (i.e., low resistance through oxide scale, and internal or surface precipitation of insulating phases), manufacturability constraints (i.e., low-cost materials, ease of fabrication, and dimensional tolerance required for stack fabrication), and design constraints (i.e., thermal conductivity). Additionally, compatibility with hydrocarbon fuels (avoiding carburization or sulfidation that will change surface properties) and tolerance to potential redox cycles on the anode side would enhance the commercial applicability.

The requirements of other metallic components, while somewhat less restrictive, are still constrained by a combination of technical, cost, and fabrication issues (e.g., the metal dusting phenomenon, wherein high carbon activity in syngas is known to pit the metal surface in a temperature range of 400 to 600 °C). Protection against sulfidation is also important for fuel gas feed tubes. The heat exchanger components must possess high-temperature oxidation resistance in both dry incoming air and in exhaust air containing potentially high steam and CO_2, as well as limit the evaporation of species such as chromium oxide to negligible amounts in order to eliminate electrode poisoning effects.

Similar constraints exist for stack gas manifold components. They must be electrically isolated from the stack in addition to having thermal expansion match to the stack and negligible volatile species.

This paper was presented at the ASM Materials Solutions Conference & Show held October 18-21, 2004 in Columbus, OH.

S. Elangovan, S. Balagopal, J. Hartvigsen, I. Bay, D. Larsen, M. Timper, and **J. Pendleton,** Ceramatec, Inc., 2425 South 900 West, Salt Lake City, UT 84119-1517. Contact e-mail: elango@ceramatec.com.

2. Alloy Selection

The most demanding component in the SOFC is the interconnect. Meeting all the requirements may be difficult in the near future as many technical issues relating to in-stack interactions, for example, the chemical and physical stability of the interconnect interface to the contact layers and chromium-poisoning effect on cathodes, are still emerging. Thus, a somewhat flexible approach is needed to demonstrate near-term stack operational goals. The two top criteria for selection are the thermal expansion match with the active components and the formation of conductive scale. The coefficient of thermal expansion (CTE) of an active cell ranges from 10 ppm/°C for zirconia to about 12 ppm/°C for the anode. The CTE of ferritic stainless steel falls within this range, while super alloy compositions range from 14 to 18 ppm/°C. Among the ferritic stainless steel compositions, the chromia formers are better suited than alumina formers because the chromia exhibits electronic conductivity. Custom alloys such as the Crofer 22 and ZMG232 as well as commercial alloys from stainless 400 series and E-brite are under investigation (Ref 2).

High-temperature components that do not require electrical properties can be made from Ni-Cr-based superalloys that form alumina such as the oxidation protection scale. These components include high-temperature sections of the air heat exchanger and pipes. In general, once the protective alumina scale is formed the volatilization of chromium oxide vapor practically ceases. Care must be taken, however, to avoid chromia evaporation during initial use. Thus, the primary motivation for alloy selection in such components is cost and manufacturability. Design options exist to construct heat exchangers using different alloys for hot and cold sections to reduce the overall cost. The secondary objectives include resistance to airborne contamination and high humidity, especially in the hot air exhaust section, and thermal cycle capability.

The fuel gas feed tubes and reformer housing are more challenging for two reasons: the presence of sulfur species in the fuel; and the metal corrosion caused by high carbon activity in fuel. The fuel may contain sulfur from potential sulfur slip from the clean-up process or when the sulfur removal subsystem is eliminated to provide system simplicity. The sections of fuel feed tubes that face the temperature range favoring the metal dusting phenomenon need to be protected.

The requirement of thermal expansion match with the stack adds restrictions to the choice of alloy materials for the stack manifold. Once again, ferritic stainless steel can be used with appropriate electrical insulation and dielectric layers where necessary. Chromium evaporation must, however, be addressed either in the selection or subsequent preparation of the manifold components. Alternatively, alumina-forming ferritic stainless steel may provide both the electrical insulation and Cr vapor barrier, after an appropriate heat treatment.

3. Experimental

For the interconnect alloy evaluation, a commercial 400 series stainless steel was selected. The selection was primarily based on the desire to have a chromium content in the range of 18 to 22%, low silicon and aluminum content, as well as availability in thin sheet forms suitable for perforation and corrugation operations. To form a continuous layer of chromia on the surface, it is essential to have chromium content higher than 12 at.%, while the upper limit is determined by the σ-phase field. As the target operating temperature of SOFCs is in the range of 650 to 700 °C, it is essential that the chromium content be well below 30 at.% to avoid the brittle σ-phase.

3.1 Surface Treatment

As the stainless steel selected for use as interconnects is a chromia former, it is expected that a conductive chromia scale will form at the SOFC operating temperature. However, to achieve the desired long-term stability of the interconnect interface, the growth rate of the oxide scale must be reduced. Thus, the initial objective of surface treatment is to reduce the scale growth rate. Considerable work was done to determine the optimal process conditions to modify the native chromia scale such that the scale growth rate is reduced. The growth rate is monitored through gravimetry. Additional results, both at Ceramatec and in the literature, have suggested that chromium evaporation from the metal interconnect surface, particularly on the cathode side, is deleterious to cathode performance and must be controlled. Thus, the second objective of the surface treatment is to reduce the chromium evaporation rate. A graded surface treatment is applied to the stainless steel coupons to achieve these objectives. The surface treatment and subsequent layer application are done using proprietary coating and heat-treating techniques to achieve a dense layer of desired phases. The first layer on top of the coupon modifies the native scale composition, while the second layer provides an $LaCrO_3$ perovskite composition. Among the various chromium compositions, $LaCrO_3$ has the lowest Cr activity and thus is expected to significantly reduce chromium volatility. The $LaCrO_3$ is also a good electronic conductor in air and thus will provide a stable and conductive layer. The conductivity of the $LaCrO_3$, however, is approximately 10 to 20 S/cm, depending on the dopant, and thus may not provide sufficient in-plane conduction. Thus, a current collection layer of higher conductive perovskite is required as the top layer. For the evaluation of coupons for various required properties, such a perovskite layer was screen-printed. Alternatively, thermal spray trials were also performed at the Idaho National Engineering and Environmental Laboratory. The thermal spray technique is expected to provide a consistent and dense layer. For the cathode-side evaluation, the current collection perovskite layer is Sr-doped $LaCoO_3$ (LSCo), while for the anode-side a nickel layer is used.

In a parallel program investigating environmental barrier coatings (EBC) for the corrosion protection of metals in a syngas environment, a coating method was developed to apply a surface oxide coating of various fine oxide powders. Sulfidation experiments were performed using a Haynes 230 alloy by exposing EBC-coated and uncoated alloy coupons for 125 h at 1050 °C. Similar sulfur exposure experiments were conducted using a surface-treated stainless alloy also for interconnect evaluation.

The primary objective of the development is to achieve a scale that exhibits a low and stable electrical resistance in a relevant atmosphere. To understand the effect of surface treatments, experiments were designed to characterize the scale via mass gain measurements, microstructure evaluation, and electrical conductivity measurements. As the interconnect faces low and high pO_2 atmospheres on opposite sides, electrical measurements were made in both single and dual atmospheres. The preliminary evaluation of the effects of fuel contaminants, for example sulfur species, was also included.

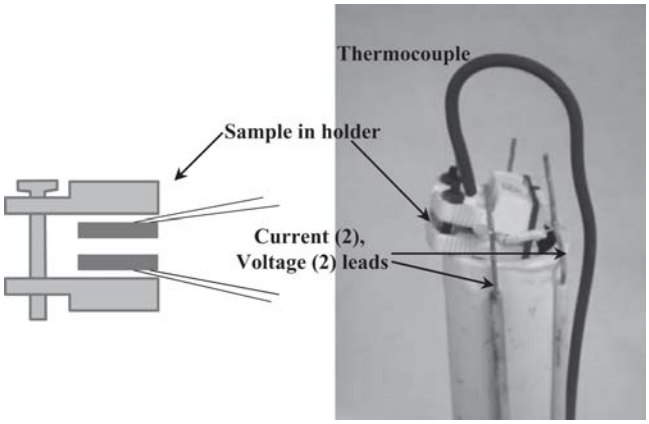

Fig. 1 Scale resistance measurement rig

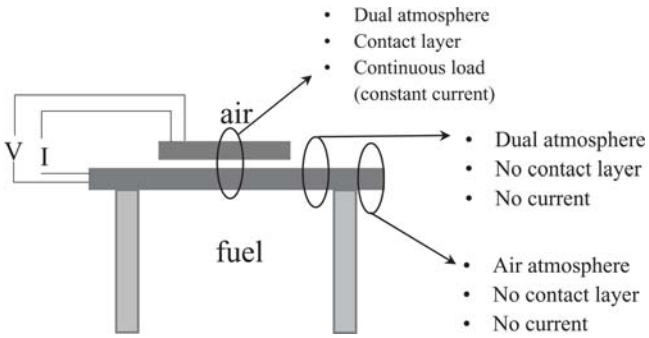

Fig. 2 Schematic of a dual-atmosphere resistance rig

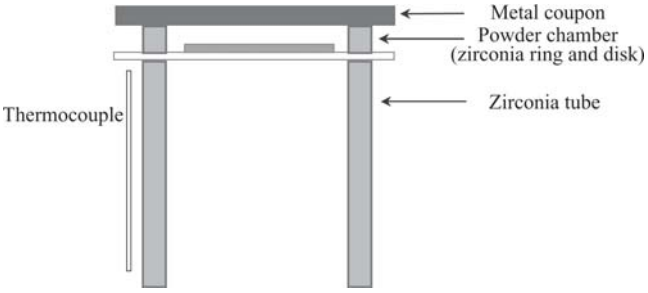

Fig. 3 Schematic of Cr evaporation test rig

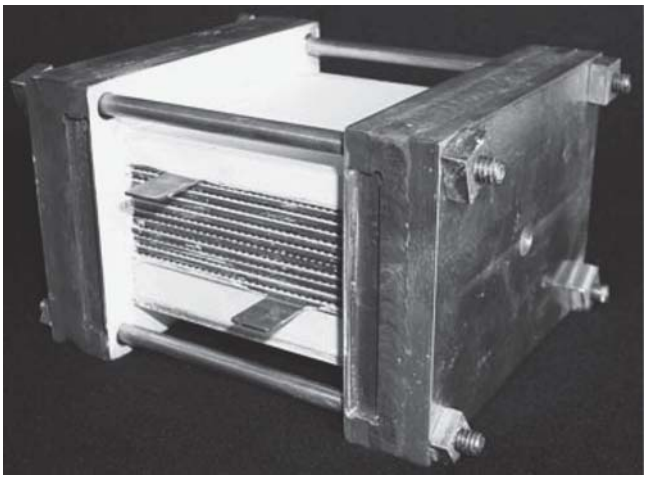

Fig. 4 Photograph of a 10-cell stack

Table 1 Test conditions for metal interconnect evaluation

Condition	Thermogravimetric analysis	Coupon couple	Dual-atmosphere couple	Stack
Atmosphere	Single	Single	Dual	Dual
Electrode and/or contact layer	No	Yes	Yes	Yes
Current	No	Intermittent; uniform current density	Continuous; uniform current density	Continuous; nonuniform current density
Temperature	Isothermal	Isothermal	Isothermal	Nonuniform distribution
Gas composition	Fixed	Fixed	Fixed	Nonuniform distribution

The mass gain measurements were monitored at 750 °C for 300 h using a thermogravimetric analyzer (model L81 TGA/DTA; Linseis Inc., Princeton Junction, NJ). The electrical resistance measurements were made using coupon couples of ~1 × 1 cm in size with surfaces of interest facing each other. An atmosphere-appropriate contact layer was used between the two coupons. The coupon couple is secured using a ceramic holder. This arrangement allows for welded current and voltage leads on the backside of the coupons such that the measurement leads do not interfere with the surfaces where the effect of scale growth is monitored. Additionally, no precious metal paste is used over the surfaces of interest. A schematic of the resistance measurement arrangement is shown in Fig. 1. The measured resistance values include the two oxide interfaces and the contact layer.

A second test rig to measure the air-side oxide scale resistance when the opposite side is exposed to a fuel atmosphere was also constructed. A disc of about 3.5 cm diameter is sealed to an alumina tube. Another smaller coupon (~1 × 1 cm) is placed on top of the larger coupon. The surfaces of interest again face each other with an LSCo contact layer electrically connecting them. The smaller coupon has current and voltage leads welded onto the backside, while the larger disc has the two welded onto the side that is exposed to air. As the fuel gas atmosphere is maintained on the inside of the tube, the resistance measurements are made through two scales exposed to air. It must be noted that the measurement lead arrangement allows the monitoring of resistance only through air-side scales without the interference of changes that may occur to fuel side scale. Additionally, this arrangement also allows examination of scale microstructure not only under the current flow region, but also where there is no electric current with the large coupon exposed dual and single air atmospheres. A schematic of the dual atmosphere, electric resistance measurement rig is shown in Fig. 2. A similar arrangement is also planned to investigate the fuel-side scale resistance under the influence of the dual atmosphere as a function of different fuels such as hydrogen and syngas as well as the effects of sulfur species.

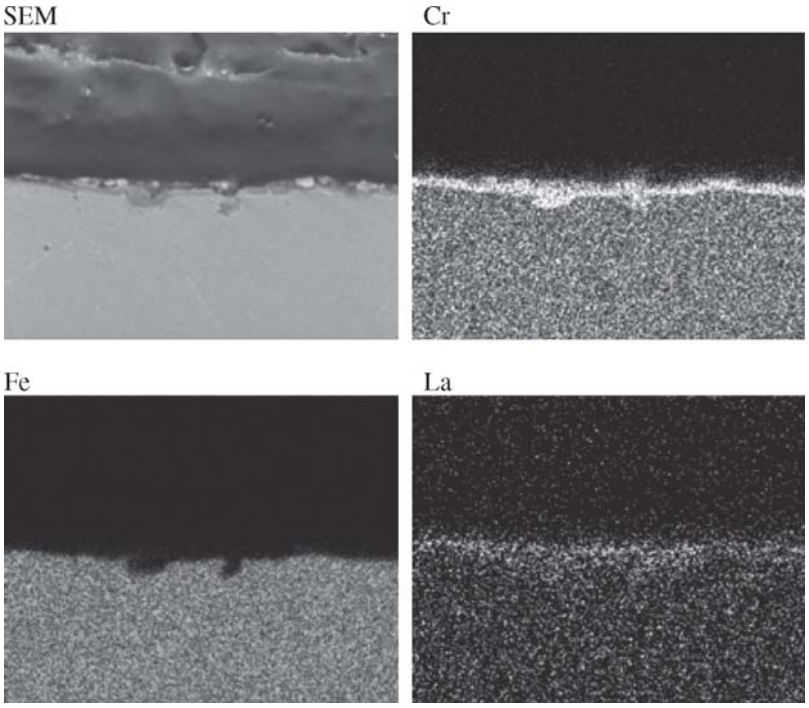

Fig. 5 Elemental maps of a surface-treated stainless steel coupon

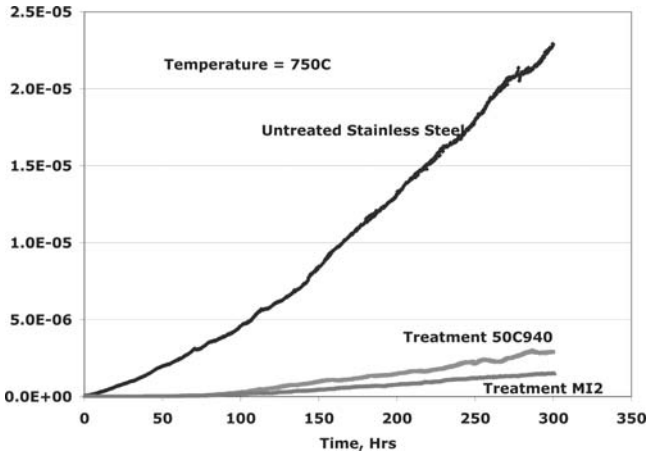

Fig. 6 Isothermal mass gain of metal coupons

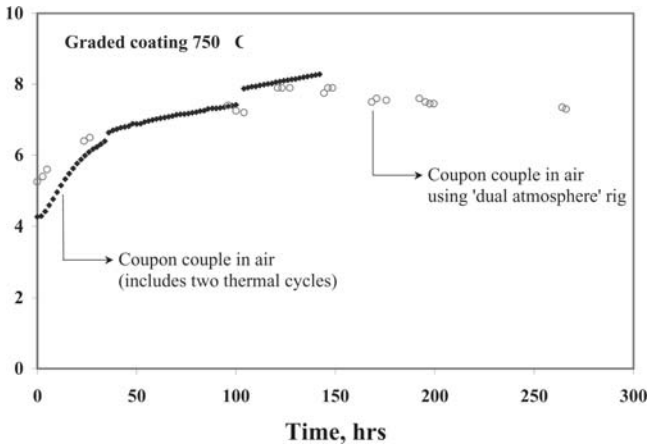

Fig. 7 Resistance of surface-treated stainless coupons

The interconnect experiences fairly complex and varying conditions during stack operation. Ideally, test conditions simulating stack operation are desired for coupon evaluation; it is difficult to achieve those conditions for all characterizations. Additionally, to understand and quantify various effects contributing to potential interconnect degradation, experiments that selectively vary test conditions are necessary. The above experiments are designed such that various interconnect parameters are characterized and quantified starting with simple test conditions and advancing to more complex ones. A comparison of test conditions of these tests and the stack conditions is shown in Table 1.

The chromia evaporation was quantified using a getter technique. The metal coupon of interest was placed at a distance of approximately 0.2 cm from a bed of a known quantity of high-purity alumina powder. The powder chamber was constructed (Fig. 3) using a zirconia disk (diameter ~ 4 cm) that was sealed to a ring of zirconia, which in turn was sealed to a long zirconia tube. The metal coupon was cemented onto the zirconia ring in four places such that a small air gap was maintained between the metal and the ring. The arrangement was maintained at 750 °C for 300 h. The exposed alumina powder was dry-milled using zirconia media to homogenize the powder. The powder was analyzed for Cr and Mn content using the inductively coupled plasma mass spectrometry.

Table 2 Analysis of alumina powder (ppm by mass)

Material	Baseline powder	Powder exposed to untreated coupon	Powder exposed to treated coupon
Cr	<0.5	250	140
Mn	<0.25	3.4	<2.5

Finally, a limited series of short stack tests was conducted to evaluate as well as to identify the technical challenges that need to be solved to develop functional metallic interconnects for SOFCs. A photograph of a 10-cell stack is shown in Fig. 4.

4. Results

4.1 Surface Treatment

The surface treatment of the coupons was done to achieve a dense initial scale that contains predominantly an $LaCrO_3$ phase as the outer layer. The results from an energy-dispersive analysis are shown in Fig. 5. The x-ray map shows the presence of La and Cr on the surface oxide layer and the absence of Fe. The x-ray diffraction analysis of the surface confirms the presence of a mixture of $LaCrO_3$ and Cr_2O_3 phases. Further process optimization might be necessary to improve the content of $LaCrO_3$, and modification to the process parameters is under way.

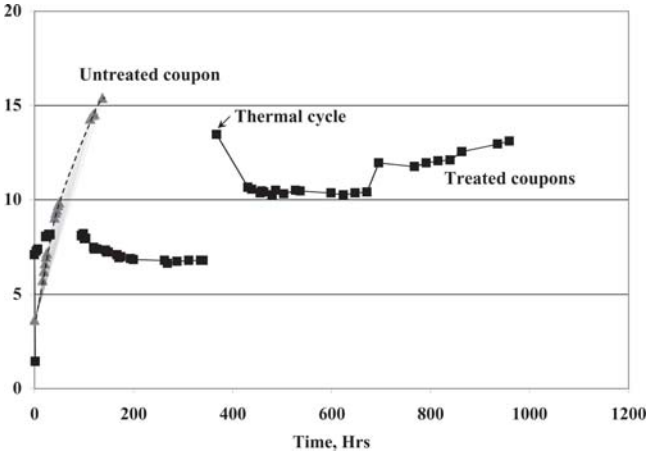

Fig. 8 Resistance of coupon couples in a dual atmosphere

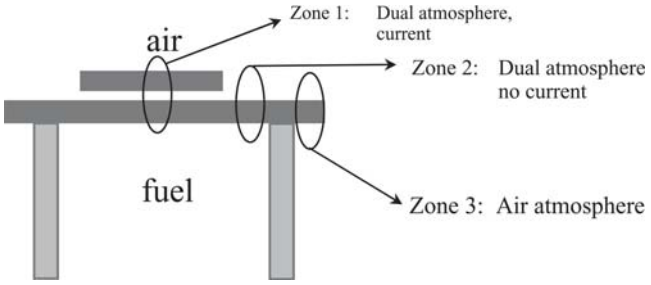

Fig. 9 The three zones of interest exposed to different test conditions

4.2 Mass Gain Measurement

Both treated and untreated coupons were tested for mass change in air at a temperature of 750 °C. The treated coupons showed a significantly lower mass gain as a function of time. The mass gain of the various coupons is shown in Fig. 6.

4.3 Chromium Evaporation

The Cr and Mn contents of the alumina powder batches are shown in Table 2. A baseline alumina powder and the powder batches exposed to untreated and surface-treated metal coupons are compared. The treatment reduces the Cr evaporation by nearly 50%. It is likely that when complete surface coverage with $LaCrO_3$ phase is achieved, a further reduction in Cr evaporation can be expected. It is also possible to achieve a similar effect when a dense, conductive perovskite layer is thermal sprayed over the treated surface. Chromium evaporation tests using surface-treated, thermal-sprayed metal coupons are planned.

4.4 Conductivity Test

The scale conductivity using coupon couples were reported earlier (Ref 3). Those measurements were made after modification to scale composition to reduce scale growth rate. Additional measurements were made after applying the graded coating on the metal coupon. The conductivity in air at 750 °C was measured using both the coupon couple technique (Fig. 1) and the dual-atmosphere test rig (Fig. 2) with air on both sides. The results are given in Fig. 7. The measured resistance values are essentially identical using both techniques, validating the dual-

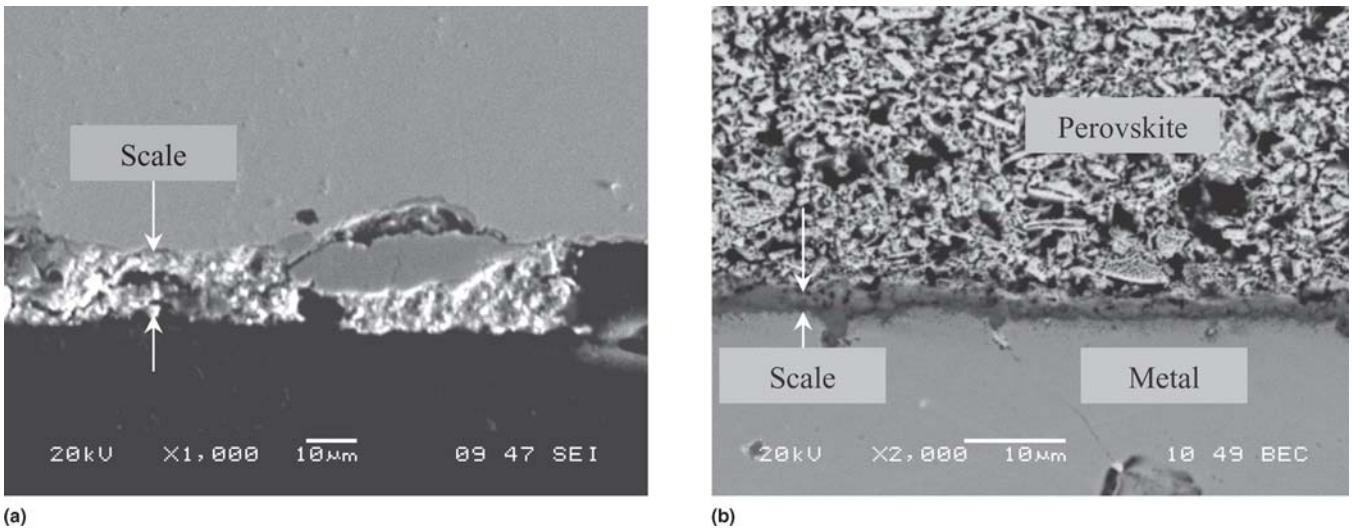

Fig. 10 The air-side scale interface of zone 1 for untreated and treated coupon couples. (a) Untreated air side of a dual atmosphere under constant current for ~ 200 h (15 μm scale, poorly bonded). (b) Treated coupon air side of a dual atmosphere under constant current for 1000 h (< 1 μm scale, well-bonded to metal)

Fig. 11 Elemental analysis of scale from zone 1 of the untreated sample

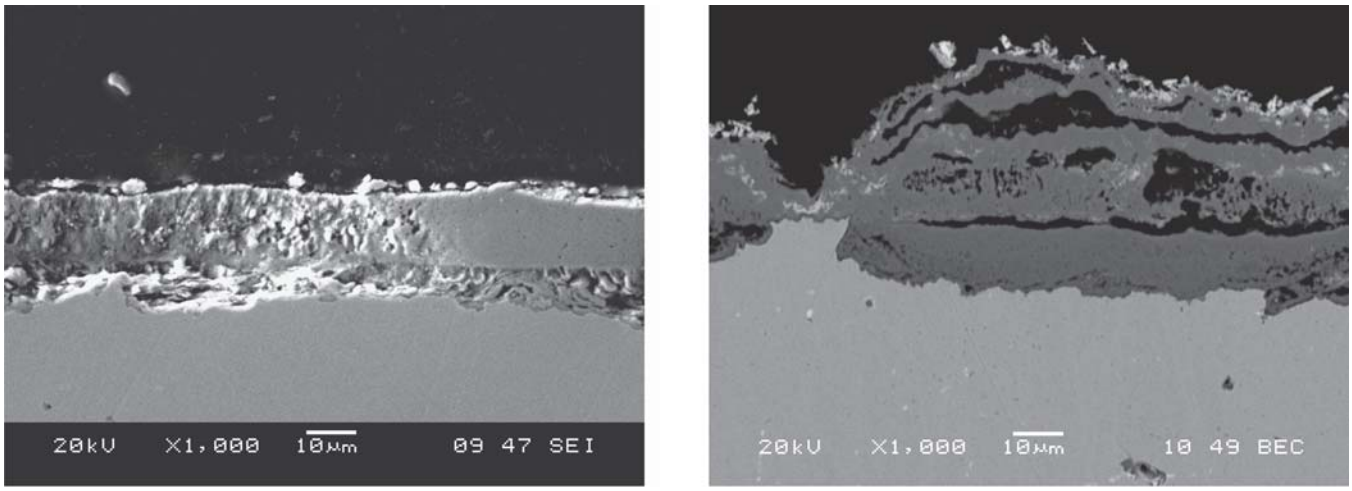

Fig. 12 The air-side scale interface of zone 2 for untreated and treated coupon couples. (a) Untreated coupon, dual atmosphere, no current, air side. (b) Treated coupon, dual atmosphere, no current, air side

atmosphere test rig for subsequent measurements with two different atmospheres across the coupon.

4.5 Dual-Atmosphere Test

Coupon sets, both surface-treated and untreated, were evaluated using the dual-atmosphere rig. A layer of LSCo was used as the contact layer between the large and small coupons. The resistance values measured for the coupon couples under the dual-atmosphere conditions are shown in Fig. 8. A constant current density of 200 mA/cm^2 was maintained during the duration of the test. As noted before, the test arrangement isolates the measurement of air-side resistance without the influence of changes to the fuel-side scale properties.

The untreated coupon couple showed a rapid increase in resistance, and the test was terminated after about 180 h. The treated coupon couple showed a stable resistance of about 8 mΩ-cm^2 up to about 400 h. After an unplanned thermal cycle, the resistance remained at about 10 mΩ-cm^2 for another 300 h, after which it showed an increase in resistance. The reason for the increase in resistance toward the end of test is not clear.

Scanning electron microscopy (SEM) of the various zones from the test coupons was conducted. The three zones of interest, dual atmosphere with continuous current (zone 1), dual atmosphere with no current (zone 2), and finally air exposure in proximity to the dual-atmosphere region (zone 3), are shown in Fig. 9.

The SEM images of the two sets of coupon couples from zone 1 are shown in Fig. 10. The untreated coupon, exposed to dual atmosphere under the constant current load for < 200 h, shows a significant scale thickness (Fig. 10a). The analysis of scale composition (Fig. 11) shows a poorly adhered Cr-rich scale with an Fe-rich overlayer. In contrast, the treated samples show a very thin oxide scale, on the order of 3 µm, even after the 1000 h exposure test under similar test conditions (Fig. 10b). Analysis shows that the scale is rich in Cr with a small amount of Fe. The scale is also bonded well to both the base metal and the LSCo contact.

A comparison of air-side scales from zones 2 and 3 are shown in Fig. 12 and 13. The scale is considerably thicker in the no-current region of the dual atmosphere for both untreated and treated coupons. The untreated coupons again show two distinct oxide layers: the layer immediately adjacent to the metal is made of a mixture of chromium oxide and iron oxide, while the top layer is made predominantly of iron oxide. The treated coupon has a scale with a mixture of chromium and iron oxides that is well adhered to the metal. However, it also shows a top layer of iron oxide that has debonded from the first scale.

Figure 13 shows (zone 3) that the treated metal has a well-

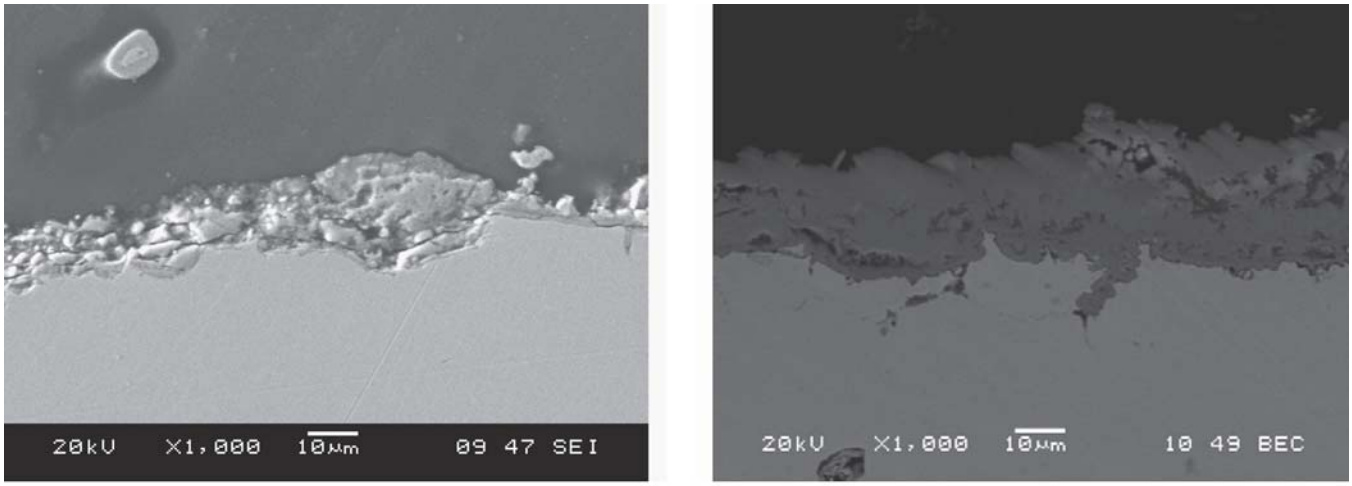

Fig. 13 The air-side scale interface of zone 3 for untreated and treated coupon couples. (a) Untreated coupon, no current, air side edge. (b) Treated coupon, no current, air side edge

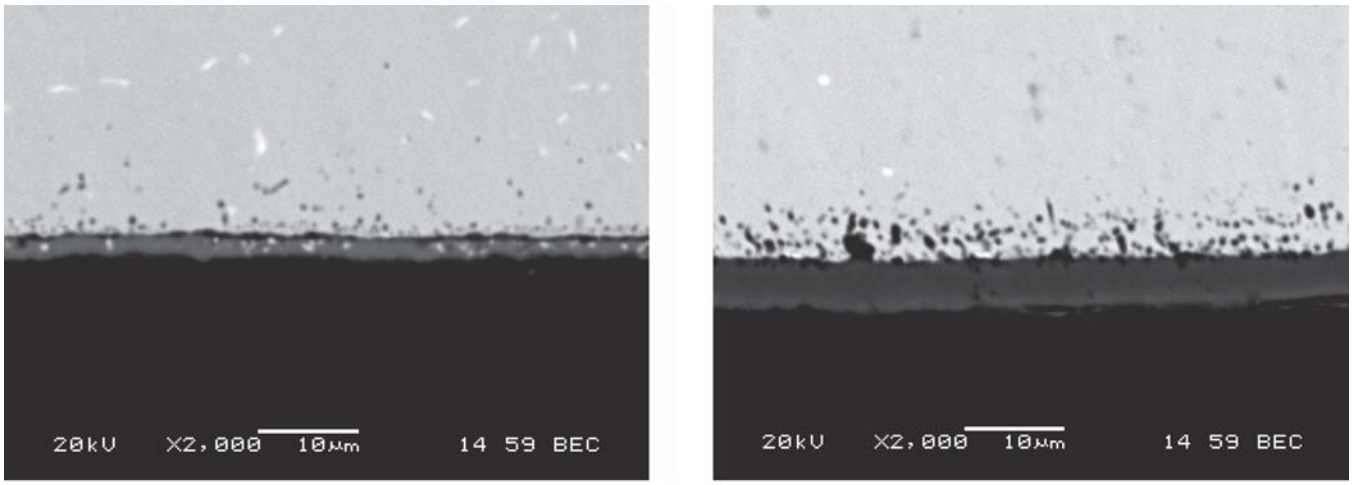

Fig. 14 Scale on fuel side. (a) Coupon exposed to syngas. (b) Coupon exposed to syngas with H_2S

bonded scale compared with the untreated metal. Both scales, however, are a mixture of chromium oxide and iron oxide. Even though zone 3 is exposed to air on both sides, the diffusion of hydrogen through the metal to affect the air-side scale cannot be discounted due to the proximity of zone 3 to zone 2.

4.6 Effect of Syngas and Sulfur

In a separate test, stainless steel coupons were exposed to syngas as well as syngas with high H_2S content (i.e., several hundred parts per million) for about 250 h. In both cases, the scale was predominantly chromium oxide. Both tests also showed porosity in the metal underneath the scale. Exposure to sulfur, however, increased the scale thickness as well the porosity in the base metal, as is seen in Fig. 14.

4.7 Coating for Nonelectrochemical Components

An oxide coating was applied on a superalloy (Haynes 230) coupon. The primary purpose of this coating is to provide an environmental barrier against corrosion in syngas. The specific composition of the coating can be modified to suit the base metal as well the exposure environment. The coating thickness has been varied from 2 to 60 μm. An SEM image of an oxide coating on Haynes alloy is shown in Fig. 15. This technique can be used to apply protective coating on metal surfaces exposed to a fuel gas atmosphere such as the fuel feed tubes.

5. Summary and Conclusions

The basic requirements for metal interconnects in SOFCs are very complex. Additionally, an understanding of the behavior of alloys in SOFC operating conditions and of the interactions among various electrochemical components proximal to interconnects is still emerging. As the operating envelope and designs of SOFC systems vary widely depending upon the intended application, additional tailoring of the properties may also be needed. Thus, the design of custom alloys to meet all requirements is quite challenging. The approach used

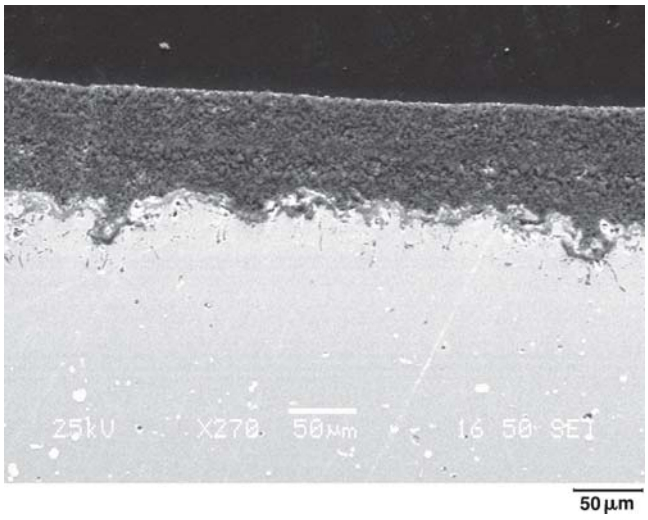

Fig. 15 An oxide coating on a Haynes 230 alloy

in our laboratory was to select and evaluate commercial stainless steel and to modify it as necessary to meet the requirements of metal interconnects.

It was determined that the commercial alloy requires surface modifications to meet the long-term performance objectives. The evaluation ranged from simple oxidation properties and electrical conductivity measurements in air to a more complex evaluation of scale growth and electrical conduction in a dual atmosphere. In general, the surface treatment option selected provides more stable oxide scale and electrical conductivity in both air and dual-atmosphere environments. It also shows a decrease in the chromium evaporation rate, as measured by a gettering technique. Additional process improvement may be needed to obtain a further reduction in the chromium evaporation rate.

Acknowledgment

This work was supported in part by the U.S. Department of Energy (DOE) Solid-State Energy Conversion Alliance Core Technology Program under Cooperative Agreement No. DE-FC2602NT41569 for SOFC interconnect development and DOE-SBIR Grant No. DE-FG02-03ER83620 for EBC development. This report was prepared as an account of work sponsored by an agency of the U.S. Government. The views and opinions of the authors expressed herein do not necessarily state or reflect those of the U.S. Government or any agency thereof.

References

1. K. Hilpert, W.J. Quadakkers, and L. Singheiser, Interconnects, Handbook of Fuel Cells - Fundamental Technology and Applications, Vol 4, W. Vielstich, A. Lamm, and H. Gasteiger, Ed., John Wiley & Sons, Ltd., West Sussex, UK, Chapter 74
2. SECA Core Technology Program, SOFC Interconnect Meeting, July 28-29, 2004, http://www.netl.doe.gov/publications/proceedings/04/seca-sofc/sofc-sofc.html
3. S. Elangovan, S. Balagopal, M. Timper, I. Bay, D. Larsen, and J. Hartvigsen, Evaluation of Ferritic Stainless Steel for Use as Metal Interconnects for Solid Oxide Fuel Cells, *J. Mater. Eng. Perf.,* 2004, **13**(3), p 265-273